Effect of Nanonization on Absorption of 301029: *Ex Vivo* and *In Vivo* Pharmacokinetic Correlations Determined by Liquid Chromatography/Mass Spectrometry

Lee Jia,[1,3] Hong Wong,[1] Cesario Cerna,[1] and Steve D. Weitman[2]

Received January 17, 2002; accepted April 9, 2002

Purpose. To compare Caco-2 monolayer permeability and *in vivo* bioavailability of microparticle with nanoparticle 301029, a thiadiazole derivative, and to determine whether nanonization could improve oral bioavailability of the poorly soluble compound.

Methods. The mean particle size of 301029 was reduced from 7 μm to 280 nm by pearl milling. In the *ex vivo* assay, both microparticle and nanoparticle 301029 at the same concentration were separately added to apical side and were collected from basolateral side of Caco-2 monolayer. In the bioavailability study, the two particle sizes of 301029 were orally administered to rats, respectively, and blood samples were collected. Nanoparticle 301029 in culture medium and rat serum was detected by a liquid chomatography-mass spectrometer (LC/MS) coupled with atmospheric pressure chemical ionization (APCI).

Results. Permeability rate and permeated amounts of nanoparticle 301029 across the Caco-2 monolayer were about four times higher than those of microparticle 301029. In a pharmacokinetic study, nanoparticle 301029 showed T_{max} about 1 h, whereas the microparticle 301029 showed T_{max} at 4 h. The C_{max} and AUC of nanoparticle 301029 were 3- to 4-fold greater than those of microparticle 301029, resulting in a significant increase in oral bioavailability of 301029 as compared with microparticle 301029. The *ex vivo* permeability and *in vivo* pharmacokinetic data indicate that nanoparticle formulation improves both absorption rate and absorption extent of the poorly soluble drug.

Conclusions. Nanoparticle formulation enhances both Caco-2 monolayer permeability and rat oral bioavailability of the poorly soluble 301029. The result also demonstrates a close correlation between *ex vivo* Caco-2 permeability model and *in vivo* gastrointestinal absorption.

KEY WORDS: nanonization; permeability; bioavailability; thiadiazole; *ex vivo-in vivo* correlation.

INTRODUCTION

301029 (Fig. 1), a representative thiadiazole derivative, was found to be a highly effective inhibitor of bovine viral diarrhea virus (BVDV). This drug candidate exhibits a therapeutic index 100-fold greater than existing approved hepatitis C virus (HCV) inhibitor, ribavirin, based on its high efficacy and low toxicity. Mechanistic studies revealed that 301029 inhibits intermediate steps in the virus replication cycle, resulting in a significant reduction in RNA synthesis. Our recent studies demonstrated that 301029 has antiviral properties against HCV and BVDV replication (unpublished observation) that would provide advantages over existing therapies using ribavirin. To develop this compound into a novel antivirus drug, we determined the pharmacokinetic profiling of oral 301029 in mice by using a liquid chromatography/mass spectrometer (LC/MS) method (1). The pilot study indicates that 301029 has relatively low bioavailability most likely due to its poor aqueous solubility (~50 μg/ml).

At present, about 10% of drugs under investigation have bioavailability problems due to poor solubility. It is estimated that about 40% of newly developed drugs will be poorly soluble in the future (2). Poor drug solubility makes it very difficult to perform high-throughput screening of compounds for potential drug effects. Therefore, there is a high need for intelligent drug formulations to achieve a sufficiently high bioavailability. Many different approaches have been developed to overcome the solubility problem of poorly soluble drugs, including solubilization, inclusion compounds, and complexation. An alternative to these methods developed was the production of drug nanoparticles by pearl milling or high-pressure homogenization. The basic principle of nanonization is the increase in surface area and concentration gradient of the poorly soluble compounds, which may lead to an increased dissolution rate of compounds according to the Noyes-Whitney equation (3) in comparison with a micronized product. In addition, the saturation solubility is also increased after nanonization. All of these may benefit oral bioavailability of poorly soluble drugs by enhancing drug transport through the gut wall into the systemic circulation.

Although nanoparticle formulation provides a plausible pharmaceutical basis for enhancing oral bioavailability and therapeutic efficacy of drugs, different formulations, drug carriers, and disease models may affect pharmacokinetic profiling and efficacy of the same drugs. For instance, liposome formulations of mitoxantrone showed the highest antitumoral effects in a leukemia model, but nanoparticles were least effective. In the B16 melanoma model, reversed results were observed: nanoparticle was the most potent, whereas liposomes were the least (4,5). Therefore, our initial attempts at developing 301029 nanoparticles were to test the hypotheses that nanonization improves oral bioavailability of poorly soluble drugs; and that there must be a rational *ex vivo* and *in vivo* correlation assuring that *in vitro* physicochemical properties and cellular permeability rate of nanoparticle 301029 will be positively proportional to the *in vivo* pharmacokinetic parameters. Because Caco-2 monolayer permeability has been widely utilized as *ex vivo* tools for prediction of human intestinal drug absorption (6,7), the present study was designed to determine differences between postsynthetic microparticle of 301029 (7 μm) and nanonized particle of 301029 (280 nm) in Caco-2 monolayer permeability and oral gastrointestinal absorption.

MATERIALS AND METHODS

Materials

301029 (FW 236.32) with molecular formula $C_9H_8N_4S_2$ (Fig. 1) was synthesized by our chemical team. The internal

[1] Institute for Drug Development/Cancer Therapy and Research Center, San Antonio, Texas 78245.
[2] Ilex Oncology, Inc., San Antonio, Texas 78245.
[3] To whom correspondence should be addressed: EPN, Rm 8042, NIH, 6130 Executive Blvd., Rockville, Maryland 20852. (e-mail: jiale2@mail.nih.gov)

0724-8741/02/0800-1091/0 © 2002 Plenum Publishing Corporation

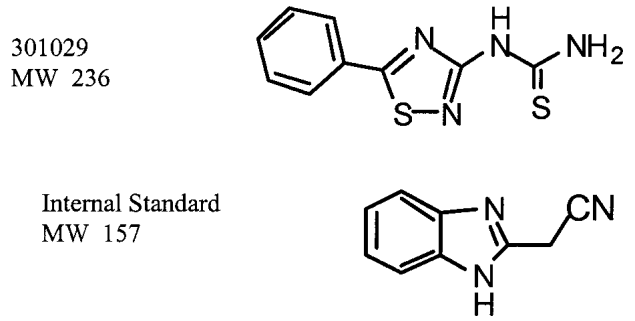

Fig. 1. Chemical structures of 301029 and the internal standard.

standard 2-benzimidazolyl-acetonitrile was purchased from Aldrich (Milwaukee, WI). Acetonitrile, methanol, chloroform, and acetic acid of HPLC grade were purchased from EM Science (Gibbstown, NJ.). *N*,*N*-dimethylformamide solution was bought from Allied Signal (Muskegon, MI). All routine culture mediums, including antibacterial agents, were purchased from Mediatech Inc. (Herndon, VA).

Preparation of Nanoparticle

Initial particle size of 301029 was 7.00 ± 0.98 μm (mean ± SD) as measured by a laser scattering particle size distribution analyzer at a scattering angle of 90° (Horiba LA-910). Microparticle 301029 powder in water was dispersed in surfactant poloxamer 407 (Pluronic F127; BASF, Mount Olive, NJ) of 1.4% (w/v) by a high-speed stirrer, and was milled at 2,200 rpm in a Netzsch media mill for 2 h at room temperature. Drug suspension was recycled though the media mill until the desired particle size was reached at 280 ± 21 nm. The suspension was diluted with water until the appropriate concentration of particle was achieved to avoid multiscattering events.

Bioanalytical Assay

Bioanalytical methods were similar to that described previously (1). Briefly, the LC/MS analysis was carried out on a Surveyor reverse-phase LC system coupled with LCQ Duo mass spectrometer (ThermoQuest-Finnigan, San Jose, CA) at ambient temperature (25°C). Separation was achieved on a 3.5 μ Kromasil C-8 column (150 × 2 mm I.D., Phenomenex, Torrence, CA) eluted with a mobile phase consisting of acetonitrile, water, and 0.01% acetic acid (90:10:0.01, v/v). Mobile phase was isocratically pumped at 100 μl/min for 6 min with the solvent front diverted to waste to prevent contamination of the mass spectrometer from the aqueous soluble salts. Vaporizer temperature was set at 200°C, the ion source corona needle voltage was set at 4.5 kV, and the sheath gas (N_2) was set at 0.5 liters/min at 100 p.s.i. The signal was amplified by adjusting the ion electron multiplier at −695 V and the dynode at −14.87 kV. The APCI mode was used to generate the positive ions. The mass selective detector was operated in the selected-ion monitoring mode to scan the 301029 ion at 237 m/z and the internal standard at 158 m/z, respectively. Quantification of 301029 was based upon ratios of peak areas to the corresponding internal standard Triplicate serum or culture medium calibration curves for 301029 were processed with each batch of samples. Curves were constructed across the concentration range of 25 to 2500 ng/ml. Quality control samples, containing 301029 at 50, 200, and 1,000 ng/ml, were processed in duplicate with each run.

Caco-2 Permeability Assay

Permeability assay was similar to that described previously (8). Human colon adenoma derived cell line, Caco-2, was purchased from American Type Culture Collection (Manassas, VA). The cells were grown in Dulbecco's modified Eagle's Medium (DMEM) and were maintained in flasks at 37°C and 5% CO_2 until cell confluence was reached. Caco-2 subculture was performed at a 1:3 ratio by using a mixture solution of 0.05% trypsin and 0.53 mM of EDTA-4Na in Hank's balanced salt solution. Appropriate amounts of cells were transferred onto clear Transwell inserts (catalogu no. 3460; Corning Costar Inc., Cambridge, MA) at a density of 10^6 cells/cm^2. The inserts feature polyester membrane filters with a pore size of 0.4 μm and a cell growth area of 1.0 cm^2. Both the membrane (10 μm thickness) and inside wall were pretreated with tissue culture medium for uniform cell attachment. Cells were maintained in a 5% CO_2 incubator at 37°C for 7 to 10 days until a monolayer was formed on the membrane. With the inserts suspended in the wells of 12-well plates, regular microparticle 301029 or nanoparticle 301029 in DMEM were added to apical chambers (total of 0.5 ml) to produce the initial 301029 concentration at 100 μM. Basolateral chambers were filled with 1.5 ml of prewarmed DMEM. To avoid the effects of drug-protein binding on the permeability rate, the DMEM was prepared without fetal bovine serum (8). Medium samples (60 μl) were then collected from basolateral chambers at 0, 0.5, 1, 2, 4, and 6 h, and were then immediately stored at −80°C until the LC/MS analysis. Transwells without cells seeded were run concurrently as a control to measure maximal permeation rate of 301029.

The apparent permeability coefficient (P_{app}) of 301029 was determined according to the following equation (8):

$$P_{app} = \frac{\Delta Q/\Delta t}{60 \cdot A \cdot C_0} \text{ (cm/sec)}$$

where $\Delta Q/\Delta t$ is the permeability rate (micromoles per second) of drug across the microporous membrane, which was calculated from the initial straight slopes. A is the surface area of membrane (i.e., 1 cm^2), and C_0 is the initial 301029 concentration (micromoles) in the apical chamber at $t = 0$. Results of the experiment performed in six replicates are presented as means ± SD.

Pharmacokinetic Experiments

Rat dosing and sampling were similar to that described previously (9,10). Briefly, Sprague-Dawley rats (135–150 g) were selected to evaluate the pharmacokinetic profiles of microparticle 301029 and its nanoparticle 301029. The rats were fasted overnight, with water being available *ad libitum*. Oral dose solutions of microparticle and nanoparticle 301029 were prepared in water containing 1.4% (w/v) of poloxamer 407. The i.v. dose solution was prepared in a vehicle of polyethylene glycol 400:saline (2:1, v/v), and was administered via tail vein. The rats were administered 301029 at 500 mg/kg and were then euthanized by CO_2 asphyxiation at the following blood sampling schedules: 0.25, 0.5, 1, 2, 4, and 8 h after oral doses; or 1 min and 0.25, 0.5, 1, 2, 4, and 8 h after the i.v. doses.

Three rats were used for each time point. Blood samples were collected and centrifuged at 5,000*g* for 10 min. The serum was collected and stored at –80°C until analysis for concentrations of 301029. One hundred microliters of serum was mixed with 100 μl of acetonitrile containing 510 ng/ml of the internal standard. After protein precipitation and centrifugation at 14,000*g* for 10 min, 20 μl of the supernatant was directly injected into the LC/MS system for analysis.

The 301029 serum concentration time curves after i.v. and oral single-dose administrations were analyzed with the WinNonlin PK software (version 3.2; Pharsight Co., Mountain View, CA), which uses a noncompartmental model for pharmacokinetic analysis (11). Calculated parameters included: T_{max}, time to maximum serum concentration; C_{max}, maximum serum concentration; $t_{1/2}$, elimination half-life; and AUC, area under the serum concentration-time curve after each single dose calculated using the linear trapezoidal rule. Bioavailability of orally administered 301029 and its nanoparticle was calculated as $(AUC_{oral}/AUC_{i.v.}) \times 100$.

Statistical Analysis

The results were expressed as mean values ± SD. The Mann-Whitney-Wilcoxon *U* test was used to investigate differences statistically when the sample size was small. However, in all statistical analysis, normality and equal variance was passed. Therefore, the one-way analysis of variance (ANOVA) was also applied to examine significance of differences, and $p < 0.05$ was considered significant.

RESULTS

Permeability of 301029 and Its Nanoparticle across Caco-2 Monolayer

The integrity of each batch of cell monolayer was first verified by microscopy, and was then tested by measuring either leakage of [^{14}C]D-mannitol in representative cell monolayer, or transmembrane resistance of the representative cell monolayer. D-Mannitol is a molecule known to traverse epithelial sheet exclusively via the paracellular route through tight junctions (zonula occludens) (12). The apical to basolateral flux for this paracellular marker did not exceed values of 0.5% penetrated per hour in this laboratory. Transmembrane resistance test revealed transcellular resistance of Caco-2 monolayer was 420 to 500 $\Omega \cdot cm^2$, whereas the cell-free membrane inserts had resistance values of 13 to 17 $\Omega \cdot cm^2$. Cell monolayer in the inserts was then confirmed as integral across the membrane and was firmly attached to the polystyrene side walls. The permeability of 301029 in microparticle and nanoparticle forms across Caco-2 monolayer is shown in Fig. 2. When applied to the apical side of Caco-2 monolayer, 301029 (100 μM) in both regular microparticle and nanoparticle formulation was detectable on the basolateral side at a time point of 30 min, indicating that 301029 is a permeable compound. Under well-controlled conditions, we found the P_{app} (centimeters per second) for nanoparticle 301029 was 2.94×10^{-6}, which was about 4-fold higher than microparticle size of 301029 (8.08×10^{-7}). Cell-free control experiments conducted in the same Transwell plate showed that the drug was freely permeable though the microporous membrane and supporting matrix. Any delay in the rate of 301029 permeability was provided by Caco-2 monolayer only. The cell-free control revealed the maximum permeation by 301029 reached a plateau of about 20 μM, which in theory was close to the final evenly distributed concentration (25 μM) of 301029 in a Transwell. Because the experiment was conducted by using the serum-free DMEM, the permeability rate of the tested drugs are comparable with each other without interference from plasma protein binding.

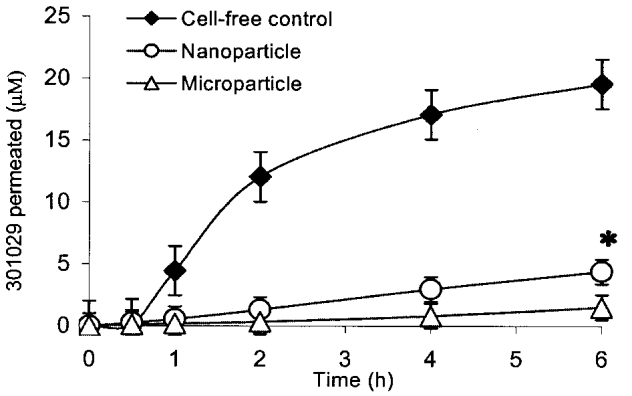

Fig. 2. Cellular permeability of regular microparticle 301029 and nanoparticle 301029 across Caco-2 monolayer. The microparticle 301029 or nanoparticle 301029 was added to the apical side of the cells, and the permeated 301029 was determined from the basolateral side by the LC/MS method. The data represents the mean ± SD (n = 6). *$p < 0.05$ compared with regular microparticle 301029 by one-way analysis of variance (ANOVA).

Single Intravenous and Oral Dose Studies in Rats

The mass spectrum of authentic 301029 in biometrics showed a protonated molecular ion (MH+) at m/z 237.0. Chromatographic peaks of 301029 in culture medium and rat serum occurred at a retention time of 9 min (Fig. 3). The 301029 identification was confirmed by mass spectrum information and comparison of retention time of 301029 with the internal standard spiked in the same preparations in the presence and absence of the biologic media. After a single i.v. injection of 301029, the serum levels of 301029 reached a maximum within 1 min, and then declined to virtually undetectable levels 8 h after the injection (Fig. 4). Maximal blood levels of 301029 after a single oral administration were reached in about 1 h for nanoparticle 301029, and in 4 h for microparticle 301029. The data indicates that nanoparticle 301029 absorbed through the gastrointestinal wall faster than microparticle 301029. In addition, nanoparticle 301029 exhibited slow clearance, but high C_{max} and AUC as compared with microparticle 301029. All these resulted in the bioavailability of nanoparticle 301029 reaching 99%, whereas microparticle 301029 exhibited 23.5%. Oral 301029 levels in rat serum declined after T_{max} with $t_{1/2}$ values comparable with those seen in rats receiving a single i.v. dose of the drug (Table I).

DISCUSSION

In the present report, both an intestinal permeability cell model and drug absorption in intact rats were used to evaluate the influence of nanoparticle formulation on the absorption and bioavailability of poorly soluble drug. Interestingly,

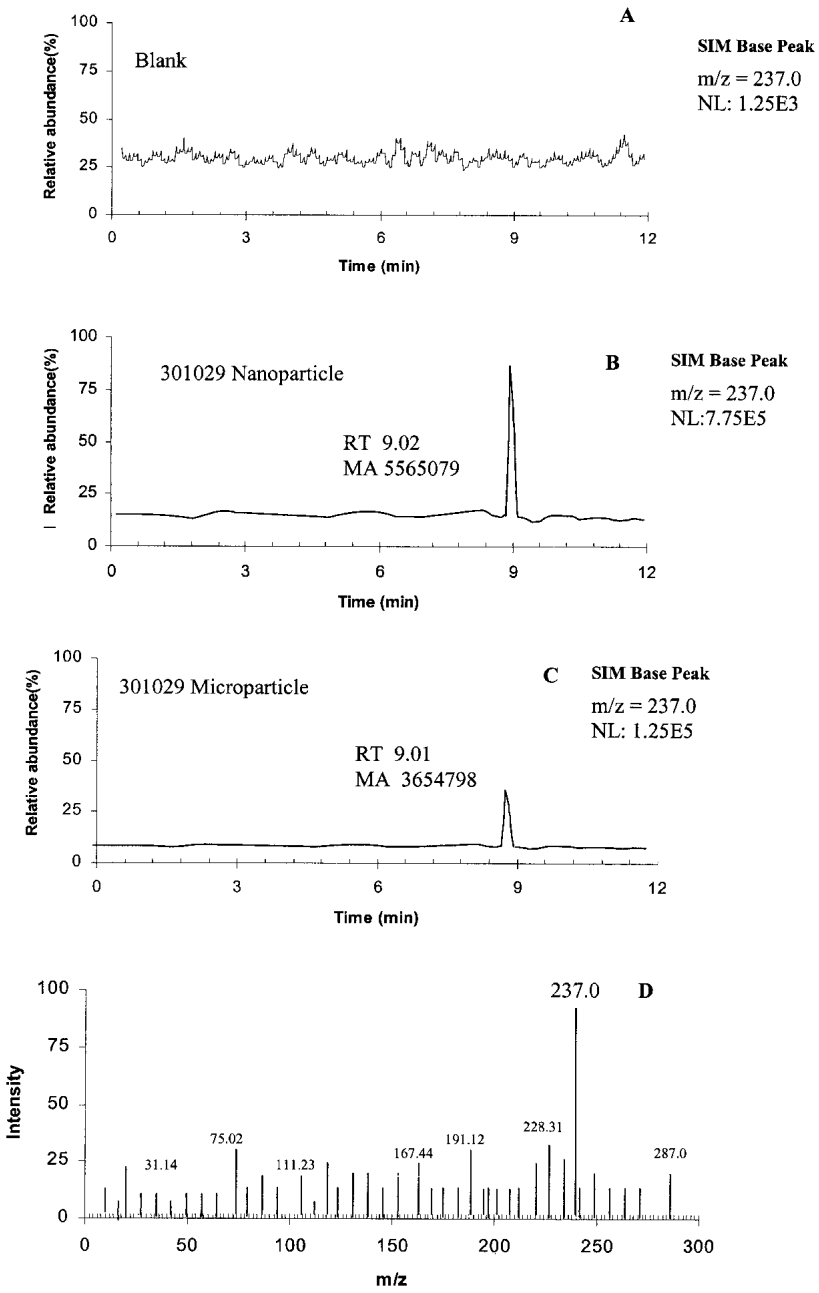

Fig 3. Representative mass chromatograms and mass spectrums of 301029 extracted from rat sera. (A) A mass chromatogram of blank serum. (B) A mass chromatogram of 301029 in nanometric size obtained from rat serum 4 h after oral dosing. (C) A mass chromatogram of 301029 in micrometric size obtained from rat serum 4 h after oral dosing. (D) Mass spectra showing positive 301029 ion at m/z 237.

the data presented here indicates that permeability across Caco-2 cells and oral bioavailability of nanoparticle 301029 was increased as compared with the larger microparticle size of 301029.

Caco-2 cells achieve a high degree of enterocytic differentiation and spontaneous dome formation, which make this cell line a more relevant *ex vivo* model for the investigation of intestinal absorption (6). Figure 2 demonstrates that permeability rate and permeated amounts of nanoparticle 301029 across the Caco-2 monolayer were about four times higher when compared with microparticle 301029. The relatively low permeability of microparticle 301029 may be due to poor solubility and slow dissolution rate of the drug in aqueous cell medium because the parallel study conducted in the same culture medium showed a significant increase in Caco-2 permeability when particle size was reduced to nanometric levels. Indeed, we observed under a microscope (×100 magnification) the undissolved 301029 particles from the micrometric formulation on the surface of the Caco-2 monolayer, whereas the 301029 particles after nanonization were hardly seen on the surface of the Caco-2 monolayer. It seems probable that the observed permeability of 301029 across the Caco-2 cells

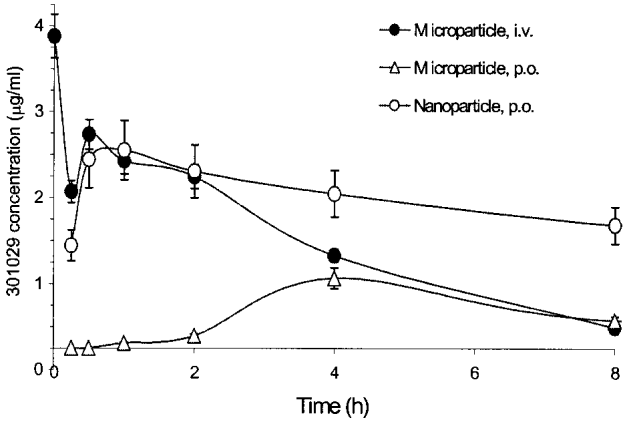

Fig 4. Serum concentration-time course of regular microparticle 301029 and nanoparticle 301029 after a single i.v. or oral administration to rats. Each point represents the mean ± SD (n = 3).

was due to passive diffusion mechanism in the present experiment because both *ex vivo* permeability and *in vivo* oral absorption 301029 was dependent on particle size and initial concentrations of the drug.

It was agreed that there was a need for much more *in vivo* pharmacokinetic data to validate *ex vivo* methods of studying drug permeability. In particular, the interplay between intestinal drug absorption and permeability remains a significant complication in interpreting data (7). Therefore, the *ex vivo* permeability kinetics of 301029 were followed up with an *in vivo* study in rats. There were marked differences in the pharmacokinetic profile between the microparticle 301029 and nanoparticle 301029. Nanoparticle 301029 was rapidly absorbed with a T_{max} of 1 h. The T_{max} for microparticle 301029 was prolonged for another 3 h. The faster absorption of 301029 after nanonization was likely due to increases in dissolution rate and saturation solubility of the drug, as well as an increased adhesiveness of nanoparticles to intestinal mucosa (see the discussion below). Nanoparticle 301029 was well absorbed, with an AUC value four times more than that of micrometric size of 301029. As can be expected, the clearance rate of nanoparticle 301029 was much lower than microparticle 301029 because clearance is more readily estimated by dividing dose by AUC. The large AUC value resulted in an oral bioavailability of 99% for nanoparticle 301029. In contrast, the microparticle 301029 obtained an oral bioavailability of 23%. The present cell permeability study supports that 301029 is a permeable drug. Therefore, the limited absorption of 301029 as a microparticle is indicative of a poorly soluble drug with bioavailability that is limited by dissolution rate, saturation solubility, and adhesiveness to the intestinal mucosa of the drug.

Nanoparticle formulation is an ideal tool for actively screening newly developed compounds that are poorly soluble. In addition, it is a tool to determine relative bioavailability of poorly soluble drugs that cannot be injected as a drug solution. Beneficial effects of drug nanonization on bioavailability are primarily based on the fundamentals that nanonization increases the surface area of poorly soluble drugs. Consequently, one can predict the following: An increase in adhesion surface area between nanoparticles and the mucin layer coating intestinal epithelium of villi facilitates the nanonized drug to traverse the mucin layer and the epithelial cells, resulting in an increase in oral absorption of the nanonized drug; compared with large particles, nanoparticles in general possess a stronger curvature of the surface, which produces more dissolution pressure with a corresponding increase in saturation solubility (13). The increase in saturation solubility, in turn, favors increased concentration gradient between intestinal epithelial cells and the mesenteric circulation beneath; and an increased dissolution velocity of the drug, which overcomes this rate-limiting step in the drug absorption process. In addition, the diffusion distance on the surface of drug nanoparticles is decreased, causing an increased concentration gradient (2). An increase in surface area and concentration gradient leads to a more pronounced increase in the dissolution rate compared with a micronized product. Saturation solubility and dissolution rate are important parameters affecting the bioavailability of orally administered drugs. Drug nanonization can reduce erratic drug absorption so the adhesion process of drug nanoparticles to mucosal surface would be highly reproducible and not very affected by the nutritional and food status of patients. It has been reported that smaller particles of drugs are taken up more easily by macrophages and obtain a higher deposition rate, and hence a better therapeutic index (14). Based on these favorable characteristics, nanonization has the potential to overcome absorption limitations of poorly soluble drugs.

CONCLUSIONS

In the present study, we investigated *ex vivo* cell permeability and *in vivo* oral absorption of 301029, a poorly soluble thiadiazole derivative, by using a Caco-2 intestinal epithelial model and intact rats to determine whether the nanonization could improve *ex vivo* cell permeability and *in vivo* oral bioavailability of 301029. LC/MS analysis of 301029 permeated the Caco-2 monolayer or absorbed into the systemic circulation revealed that nanonization of 301029 particle signifi-

Table I. Pharmacokinetic Parameters of Nanoparticle and Microparticle 301029 after Single i.v. or p.o. Administration to Sprague-Dawley Rats at 500 mg/kg (n = 18–21 rats/group)

Particle sizes	Nanoparticle (280 nm)	Microparticle (7 μm)	Microparticle (7 μm)
Dosing routes	p.o.	p.o.	i.v.
Half-life (h)	26.6 ± 0.5	24.9 ± 0.3	23.2 ± 0.7
T_{max} (h)	1.0 ± 0.2	4.0 ± 0.1	Instant
C_{max} (μg/ml)	2.30 ± 0.12	0.82 ± 0.05	3.63 ± 0.23
$AUC_{0\rightarrow 8\ h}$ (μg mL^{-1} h^{-1})	14.17 ± 0.03	3.36 ± 0.09	14.30 ± 0.14
Clearance (ml/min)	30.0 ± 0.7	121.0 ± 0.9	29.0 ± 0.3
Bioavailability (%)	99.1	23.5	–

cantly increased both the rate and amount of 301029 permeated the Caco-2 monolayer or absorbed into the systemic circulation. The present data also showed a good correlation between the *ex vivo* Caco-2 model and *in vivo* oral absorption of the drug. The size-dependent permeability and bioavailability should be given particular consideration in the development of potent and selective drug candidates with poor aqueous solubility.

REFERENCES

1. H. Wong, L. Jia, J. B. Camden, and S. D. Weitman. Liquid chromatography-mass spectrometry assay of a thiadiazole derivative in mice: application to pharmacokinetic studies. *J. Chromatogr.* **765**:55–62 (2001).
2. M. Radtke. Pure drug nanoparticles for the formulation of poorly soluble drugs. *New Drugs* **3**:62–68 (2001).
3. A. Noyes and W. Whitney. The rate of solution of solid substances in their own solutions. *J. Am. Chem. Soc.* **19**:930–934 (1897).
4. P. Beck, J. Kreuter, R. Reszka, and I. Fichtner. Influence of polybutylcyanoacrylate nanoparticles and liposomes on the efficacy and toxicity of the anticancer drug mitoxantrone in murine tumor models. *J. Microencapsul.* **10**:101–114 (1993).
5. R. Reszka, P. Beck, I. Fichtner, M. Hentschel, J. Richter, and J. Kreuter. Body distribution of free, liposomal and nanoparticle-associated mitoxantrone in B16-Melanoma-bearing mice. *J. Pharmacol. Exp. Ther.* **280**:232–237 (1997).
6. K. L. Audus, R. L. Bartel, I. J. Hidalgo, and R. T. Borchardt. The use of cultured epithelial endothelial cells for drug transport and metabolism studies. *Pharm. Res.* **7**:435–451 (1990).
7. G. T. Tucker, J. B. Houston, and S. M. Huang. Optimizing drug development: strategies to assess drug metabolism/ transporter interaction potential-toward a consensus. *Pharm. Res.* **18**:1071–1080 (2001).
8. L. Jia and H. Wong. In vitro and in vivo assessment of cellular permeability and pharmacodynamics of *S*-nitrosylated captopril, a nitric oxide donor. *Br. J. Pharmacol.* **134**:1697–1704 (2001).
9. L. Jia, X. Young, and W. Guo. Physicochemistry, pharmacokinetics and pharmacodynamics of *S*-nitrosocaptopril crystals, a new nitric oxide donor. *J. Pharm. Sci.* **88**:981–986 (1999).
10. L. Jia, M. Garza, H. Wong, D. Reimer, T. Redelmeier, J. B. Camden, and S. D. Weitman. Pharmacokinetic comparison of intravenous carbendazim and remote loaded carbendazim liposomes in nude mice. *J. Pharm. Biom. Anal.* **28**:65–72 (2002).
11. L. Jia, M. D. Linnik, and R. M. Jack. and L. Yu. Biostability and pharmacokintics of LJP 920, an octameric Gal (α1-3) Gal conjugate for the inhibition of xenotransplantation rejection. *J. Pharm. Pharmacol.* **53**:999–1005 (2001).
12. J. M. Mullin, L. Fluk, and A. Kleinzeller. Basolateral transport and transcellular flux of methyl α-D-glucoside across LLC-PK1 renal epithelial cells. *Biochim. Biophys. Acta* **885**:233–239 (1986).
13. R. H. Müller and B. H. L. Böhm. Nanosuspensions. In R.H. Müller, S. Benita, and B.H.L. Böhm (eds.), *Emulsions and Nanosuspensions for the Formulation of Poorly Soluble Drugs*, Medpharm Scientific Publishers, Stuttgart, Germany, 1998 pp. 149–174.
14. A. Lamprecht, U. Schafer, and C. M. Leh. Size-dependent bioadhesion of micro- and nanoparticle carriers to the inflamed colonic mucosa. *Pharm. Res.* **18**:788–791 (2001).